

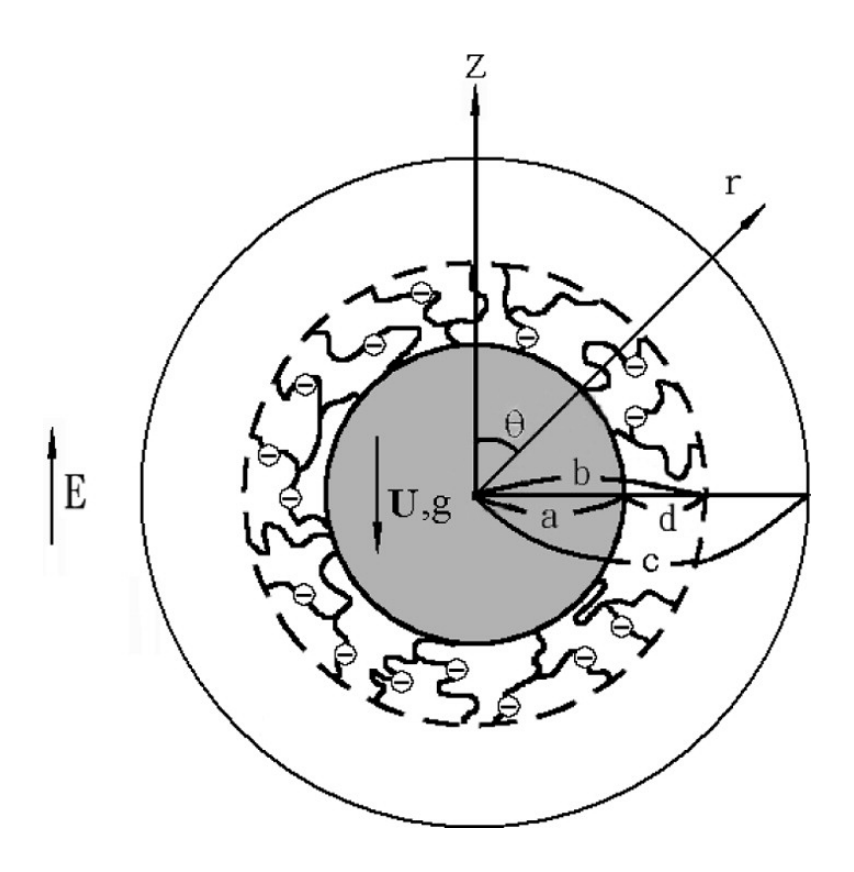


## Research Article

# Sedimentation of a Composite Particle in a Spherical Cavity

Eric Lee, Tzu-Hao Huang, and Jyh-Ping Hsu *Langmuir*, **2005**, 21 (5), 1729-1737 • DOI: 10.1021/la0476229

Downloaded from http://pubs.acs.org on November 21, 2008



### **More About This Article**

Additional resources and features associated with this article are available within the HTML version:

- Supporting Information
- Access to high resolution figures
- Links to articles and content related to this article
- Copyright permission to reproduce figures and/or text from this article

View the Full Text HTML



# Sedimentation of a Composite Particle in a Spherical Cavity

Eric Lee, Tzu-Hao Huang, and Jyh-Ping Hsu\*

Department of Chemical Engineering, National Taiwan University, Taipei, Taiwan 10617 Received September 24, 2004. In Final Form: November 16, 2004

The boundary effect on the sedimentation of a colloidal particle is investigated theoretically by considering a composite sphere, which comprises a rigid core and an ion-penetrable membrane layer, in a spherical cavity. A pseudo-spectral method is adopted to solve the governing electrokinetic equations, and the influences of the key parameters on the sedimentation behavior of a particle are discussed. We show that both the qualitative and quantitative behaviors of a particle are influenced significantly by the presence of the membrane layer. For example, if the membrane layer is either free of fixed charge or positively charged and the surface potential of the rigid core is sufficiently high, the sedimentation velocity has a local minimum and the sedimentation potential has a local maximum as the thickness of the double layer varies. These local extrema are not observed when the membrane layer is negatively charged. If the double layer is thin, the influence of the fixed charge in the membrane layer on the sedimentation potential is inappreciable.

#### Introduction

Sedimentation is one of the important phenomena of a colloidal dispersion in a gravitational field. Although it has been studied extensively and relevant results are ample in the literature, the result under general conditions has not been reported. In a study of the sedimentation of an isolated, rigid sphere under the conditions of an infinitely thin double layer, Smoluchowski<sup>1</sup> showed that the sedimentation velocity of a charged particle is much smaller than that of the corresponding uncharged particle. Booth<sup>2</sup> estimated the sedimentation velocity and the sedimentation potential of a sphere with an arbitrary double-layer thickness. His analysis was extended by Saville<sup>3</sup> to a more general case. Sedimentation is similar to electrophoresis, where an applied electric field provides the driving force for the movement of a charged particle. de Groot et al.4 found that the scaled sedimentation potential in sedimentation correlates with the electrophoresis mobility in electrophoresis, the so-called Onsager relation. Ohshima et al.<sup>5</sup> derived analytical expressions for the sedimentation potential and sedimentation velocity for the case of low surface potential and thin double layer. A thorough review for sedimentation was provided by Deen et al. Based on Kuwabara's cell model, Levine et al. were able to derive both the sedimentation potential and sedimentation velocity of a colloidal dispersion. An Onsager relation for a concentrated suspension was derived by Ohshima.<sup>8</sup> Pujar and Zydney<sup>9</sup> evaluated the sedimentation velocity of a charged particle in a spherical cavity

\* To whom correspondence should be addressed. Tel: 886-2-23637448. Fax: 886-2-23623040. E-mail: jphsu@ntu.edu.tw.

(1) Smoluchowski, M. Handbuch der Elecktrizitat und des Magnetismus; Graetz, L., Ed.; Barth: Leipzig, 1921; Vol. II. (2) Booth, F. J. Chem. Phys. 1954, 22, 1956.

under the conditions of small Peclet number and low surface potential. Their analysis was extended by Lee et al.<sup>10</sup> to the case of arbitrary electrical potential.

Nonrigid particles are often encountered in practice. For instance, biological entities such as cells and microorganisms can be mimicked by a composite particle, which comprises a rigid core and a porous or ion-penetrable membrane layer. The particles in a stable colloidal dispersion are another typical example where the surface of a particle is usually covered by surfactant molecules. In contrast to a rigid particle where the charge it carries is mainly on its surface, the charge of a composite particle comprises that on the surface of its rigid core and that arising from the dissociation of the functional groups in its membrane layer. A human blood cell, for example, has an ~15 nm thick glycoprotein layer near its surface which carries net negative charge under normal conditions.<sup>11</sup> The influence of the membrane layer of a composite particle on its sedimentation is twofold. The hydrodynamic drag that arises from the flow of the liquid inside tends to retard its sedimentation. On the other hand, the charge it carries can accelerate its sedimentation. Several attempts have been made to analyze the sedimentation of composite particles. Keh and Liu, 12 for instance, derived an analytic expression for both sedimentation potential and sedimentation velocity in a dilute suspension under the conditions of low electrical potential. The sedimentation of a concentrated suspension of porous particles was analyzed by Ohshima, 13 and analytic expressions for both sedimentation potential and sedimentation velocity were derived for the case of low electrical potential.

In this study, the boundary effect on sedimentation is investigated by considering the sphere-in-spherical cavity geometry of Pujar and Zydney.9 We extend their analysis to the case of a composite particle at arbitrary electrical potentials. Note that the result for a rigid particle can be recovered from the present study as a limiting case where the thickness of the membrane layer approaches zero. A psuedospectral method based on Chebyshev polynomials

 <sup>(3)</sup> Saville, D. A. Adv. Colloid Interface Sci. 1982, 16, 267.
 (4) de Groot, S. R.; Mazur, P.; Overbeek, J. Th. G. J. Chem. Phys. 1952, 20, 1825

<sup>(5)</sup> Ohshima, H.; Healy, T. W.; White, L. R.; O'Brien, R. W. J. Chem. Soc., Faraday Trans. 2 1984, 80, 1299.

<sup>(6)</sup> Deen, W. M.; Bohrer, M. P.; Epstein, N. B. Am. Inst. Chem. Eng. J. 1987, 27, 952.

<sup>(7)</sup> Levine, S.; Neale, G. H.; Epstein, N. J. Colloid Interface Sci. 1976, 57, 424.

<sup>(8)</sup> Ohshima, H. J. Colloid Interface Sci. 1998, 208, 295.

<sup>(9)</sup> Pujar, N. S.; Zydney, A. L. Am. Inst. Chem. Eng. J. 1996, 42,

<sup>(10)</sup> Lee, E.; Yen, C. B.; Hsu, J. P. J. Phys. Chem. B 2000, 104, 6815. (11) Seaman, G. V. *The Red Blood Cells*; Sergenor, D. M., Ed.; Academic Press: New York, 1975; Vol. 2, pp 1136–1229.

(12) Keh, H. J.; Liu, Y. C. *J. Colloid Interface Sci.* 1997, 195, 169.

<sup>(13)</sup> Ohshima, H. J. Colloid Interface Sci. 2000, 229, 140.

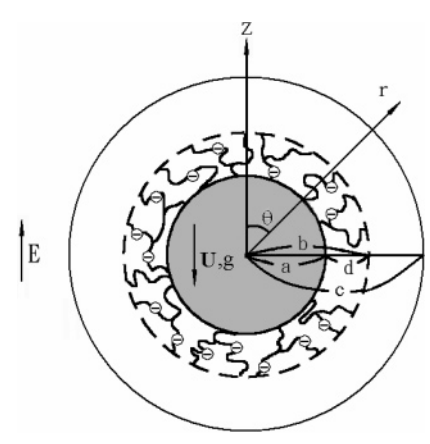


**Figure 1.** Sedimentation of a spherical particle of radius b at the center of a spherical cavity of radius c. The particle comprises a rigid core of radius a and an ion-penetrable membrane layer of thickness d. **U** is the sedimentation velocity. The deformation of the ionic cloud surrounding the particle yields an induced electric field  $\mathbf{E}$ .  $(r,\theta,\varphi)$  are the spherical coordinates with their origin at the center of the particle, and the axis  $\theta=0$  is parallel to both  $\mathbf{U}$  and  $\mathbf{E}$ .

is employed to solve the governing equations and the associated boundary conditions. The influences of the key parameters of the present problem, including the surface potential of the rigid core of a particle, the charge density in the membrane layer, the thickness of the double layer, and the relative magnitude of the particle, on its sedimentation behavior are examined through numerical simulations.

#### **Theory**

Referring to Figure 1, we consider the sedimentation of a spherical particle of radius b at the center of a spherical cavity of radius c. The particle comprises a rigid core of radius a and an ion-penetrable membrane layer of thickness d, b = a + d. The membrane layer contains uniformly distributed fixed charge. The cavity is filled with an incompressible Newtonian liquid of constant physical properties containing  $z_1$ : $z_2$  electrolyte,  $z_1$  and  $z_2$ being respectively the valences of cations and anions. Let U be the sedimentation velocity of the particle. The deformation of the ionic cloud surrounding the particle yields an induced electric field E. The spherical coordinates  $(r,\theta,\varphi)$  are adopted with their origin located at the center of the particle, and the axis  $\theta = 0$  is parallel to both **U** and **E**. Let  $z_2 = -\alpha z_1$  and  $H = (b/c)^3$ . Suppose that the system is at a quasi-steady state.

For the present case, the electric field is described by

$$\nabla^2 \phi = -\frac{\rho + \rho_{\text{fix}}}{\epsilon} \qquad a < r < b \tag{1}$$

$$\nabla^2 \phi = -\frac{\rho}{\epsilon} \qquad b < r < c \tag{2}$$

Here,  $\rho = \sum_j n_j z_j e$  is the space charge density of mobile ions,  $\nabla^2$  is the Laplace operator,  $\epsilon$ ,  $\rho$ , and  $\rho_{\rm fix}$  are respectively the permittivity of the electrolyte solution, the density of mobile ions, and the fixed charged density in the membrane layer. e and  $\phi$  are respectively the elementary charge and the electrical potential, and  $n_j$  and  $z_j$  are respectively the number concentration and the valence of ionic species j. The conservation of ionic species j leads to

$$\nabla^2 n_j + \frac{z_j e}{kT} (\nabla n_j \cdot \nabla \phi + n_j \nabla^2 \phi) - \frac{1}{D_i} \mathbf{v} \cdot \nabla n_j = 0 \quad (3)$$

where  $\nabla$  is the gradient operator,  $D_j$  is the diffusivity of ionic species j, k is the Boltzmann constant, T is the absolute temperature, and  $\mathbf{v}$  is the liquid velocity.

The flow field can be described by

$$\nabla \cdot \mathbf{v} = 0 \tag{4}$$

$$-\nabla p + \eta \nabla^2 \mathbf{v} - \rho \nabla \phi - \gamma \mathbf{v} = 0 \qquad a < r < b \quad (5)$$

$$-\nabla p + \eta \nabla^2 \mathbf{v} - \rho \nabla \phi = 0 \qquad b < r < c \tag{6}$$

In these expressions, p and  $\eta$  are respectively the pressure and the viscosity, and  $\gamma$  is the frictional coefficient of the membrane layer.

Similar to the treatment of O'Brien and White<sup>14</sup> for the case of electrophoresis, the electrical potential  $\phi$  is decomposed into the electrical potential arising from the presence of the particle or the equilibrium potential  $\phi_1$  and that induced by its sedimentation,  $\phi_2$ ; that is,  $\phi = \phi_1 + \phi_2$ . The deformation of the ionic cloud surrounding the particle can be described by expressing  $n_i$  as

$$n_j = n_{j0} \exp\left(-\frac{z_j e(\phi_1 + \phi_2 + g_j)}{kT}\right)$$
  $j = 1,2$  (7)

where  $g_j$  and  $n_{j0}$  are respectively a perturbed potential and the bulk concentration of ionic species j. Combining eqs 1, 2, and 7 yields

$$\nabla^2 \phi_1 = -\sum_{j=1}^2 \frac{z_j e n_{j0}}{\epsilon} \exp \left( -\frac{z_j e \phi_1}{kT} \right) - \frac{\rho_{\text{fix}}}{\epsilon} \qquad \alpha < r < b \quad (8)$$

$$\nabla^2 \phi_1 = -\sum_{i=1}^2 \frac{z_j e n_{j0}}{\epsilon} \exp\left(-\frac{z_j e \phi_1}{kT}\right) \qquad b < r < c \quad (9)$$

Also, it can be shown that

$$\begin{split} \nabla^2 \phi_2 &= \nabla^2 \phi - \nabla^2 \phi_1 = \\ &- \sum_{j=1}^2 \frac{z_j e n_{j0}}{\epsilon} \left( \exp \left( -\frac{z_j e (\phi_1 + \phi_2 + g_j)}{kT} \right) - \exp \left( -\frac{z_j e \phi_1}{kT} \right) \right) \end{split} \tag{10}$$

Substituting eq 7 into eq 3 yields

$$\begin{split} \nabla^2 g_j - \frac{z_j e}{kT} \nabla \phi_1 \boldsymbol{\cdot} \nabla g_j = \\ \frac{1}{D_i} \mathbf{v} \boldsymbol{\cdot} \nabla \phi + \frac{1}{D_j} \mathbf{v} \boldsymbol{\cdot} \nabla g_j + \frac{z_j e}{kT} \nabla \phi_2 \boldsymbol{\cdot} \nabla g_j + \frac{z_j e}{kT} \nabla g_j \boldsymbol{\cdot} \nabla g_j \end{split} \tag{11}$$

The pressure terms in eqs 5 and 6 can be eliminated by taking curl on both sides and applying the equation of continuity, eq 4. The analysis can be simplified further by adopting a stream function representation. After these treatments, eqs 5 and 6 become

$$E^{4}\psi - \gamma E^{2}\psi = -\frac{\sin \theta}{\eta} \nabla \times \left[\rho \nabla (\phi_{1} + \phi_{2})\right] \qquad \alpha < r < b \tag{12}$$

$$E^4 \psi = -\frac{\sin \theta}{\eta} \nabla \times [\rho \nabla (\phi_1 + \phi_2)] \qquad b < r < c \quad (13)$$

where  $\psi$  is the stream function,  $E^4 = E^2 E^2$ , and

<sup>(14)</sup> O'Brien, R. W.; White, L. R. J. Chem. Soc., Faraday Trans. 2 1978, 74, 1607.

$$E^{2} = \frac{\partial}{\partial r^{2}} + \frac{\sin \theta}{r^{2}} \frac{\partial}{\partial \theta} \left( \frac{1}{\sin \theta} \frac{\partial}{\partial \theta} \right)$$

Note that the r- and the  $\theta$ -component of the liquid velocity,  $v_r$  and  $v_\theta$ , can be expressed respectively by

$$v_r = -\frac{1}{r^2 \sin \theta} \frac{\partial \psi}{\partial \theta}$$

and

$$v_{\theta} = \frac{1}{r \sin \theta} \frac{\partial \psi}{\partial r}$$

**Boundary Conditions.** We assume that the surface of the rigid core of a particle remains at constant potential  $\zeta_a$  and that of the cavity remains at  $\zeta_b$ . Also, both the electrical potential and the electric field are continuous on the membrane layer—liquid interface. Therefore, the boundary conditions associated with  $\phi_1$  are

$$\phi_1 = \zeta_a \qquad r = a \tag{14}$$

$$\phi_1|_{r=b^{-}} = \phi_1|_{r=b^{+}} \qquad r=b \tag{15}$$

$$\frac{\partial \phi_1}{\partial r}|_{r=b} = \frac{\partial \phi_1}{\partial r}|_{r=b} \qquad r=b \tag{16}$$

$$\phi_1 = \xi_b \qquad r = c \tag{17}$$

The following boundary conditions are assumed for  $\phi_2$ :

$$\frac{\partial \phi_2}{\partial r} = 0 \qquad r = a \tag{18}$$

$$\phi_2|_{r=b^-} = \phi_2|_{r=b^+} \qquad r = b \tag{19}$$

$$\frac{\partial \phi_2}{\partial r}|_{r=b^{-}} = \frac{\partial \phi_2}{\partial r}|_{r=b^{+}} \qquad r=b \tag{20} \label{eq:20}$$

$$\frac{\partial \phi_2}{\partial r} = -E_z \cos \theta \qquad r = c \tag{21}$$

Equation 18 arises from the fact that the rigid core of a particle is nonconductive and impermeable to ion species. Equations 19 and 20 imply that both the electrical potential and the electric field are continuous on the membrane layer—liquid interface. The last expression states that the electric field on the cavity surface is that arising from the sedimentation of the particle, where  $E_z$  is the strength of the induced electric field in the z-direction.

Suppose that the rigid core of a particle is impermeable to ionic species, and both the concentration of an ionic species and its flux are continuous on the membrane layer—liquid interface. Also, the concentration of ionic species reaches its bulk value on the cavity surface. These lead to the following boundary conditions:

$$\mathbf{f_i} \cdot \mathbf{n} = \mathbf{f_i} \cdot \boldsymbol{\delta_r} = 0 \qquad r = a \tag{22}$$

$$n_j|_{r=b} = n_j|_{r=b^+} \qquad r = b$$
 (23)

$$\mathbf{f_j}|_{r=b^{-}} = \mathbf{f_j}|_{r=b^{+}} \qquad r = b \tag{24}$$

$$n_i = n_{i0} \qquad r = c \tag{25}$$

In these expressions,  $\mathbf{f_j}$  is the flux of ionic species j,  $\mathbf{n}$  is the unit normal vector, and  $\boldsymbol{\delta_r}$  is the unit vector in the r-direction.

We assume that both the rigid core of a particle and the surface of the cavity are no-slip, and both the velocity of the liquid and its normal and tangential stresses are continuous on the membrane layer—liquid interface. Therefore, the boundary conditions for the flow field are

$$v_r = U \cos \theta$$
  $v_\theta = -U \sin \theta$   $r = a$  (26)

$$v_r|_{r=b^-} = v_r|_{r=b^+}$$
  $v_\theta|_{r=b^-} = v_\theta|_{r=b^+}$   $r = b$  (27)

$$\begin{aligned} \sigma_{r\theta}^{H}|_{r=b^{-}} &= \sigma_{r\theta}^{H}|_{r=b^{+}} & \sigma_{rr}^{T}|_{r=b^{-}} &= \sigma_{rr}^{T}|_{r=b^{+}} \\ & \sigma_{rr}^{E}|_{r=b^{-}} &= \sigma_{rr}^{E}|_{r=b^{+}} & r = b \end{aligned} \tag{28}$$

$$v_r = 0 \qquad v_\theta = 0 \qquad r = c \tag{29}$$

In these expressions,  $\sigma^H$  and  $\sigma^E$  are respectively the hydrodynamic stress tensor and the Maxwell stress tensor, and  $\sigma^T = \sigma^H + \sigma^E$  is the total stress tensor.

For a simpler treatment, the governing equations and the associated boundary conditions are rewritten in dimensionless forms in subsequent discussions. To this end, the following characteristic variables are adopted: the radius of the rigid core of a particle a, the surface potential on the rigid core of the particle  $\zeta_a$ , the bulk number concentration of ionic species j  $n_{j0}$ , and the characteristic velocity  $U_E = \epsilon \zeta_a^2 / \eta a$ . We define the following dimensionless symbols: the scaled radial distance  $r^* =$ r/a, the scaled number concentration of ionic species j,  $n_i^*$ =  $n_j/n_{j0}$ , the scaled electric field  $E_Z^* = E_Z/(\zeta_a/a)$ , the scaled velocity  $v^* = v/U_E$ , the scaled sedimentation velocity  $U^*$  $=U/U_E$ , the scaled equilibrium potential  $\phi_1^*=\phi_1/\zeta_a$ , the scaled perturbed potential,  $\phi_2^* = \phi_2/\zeta_a$ , the scaled perturbed potential  $g_i^* = g_j/\zeta_a$ , j = 1,2, and the scaled stream function  $\psi^* = \psi/U_E a$ .

Because the induced electric field arising from the sedimentation of a particle is much weaker than that arising from the presence of the particle,  $\phi_2 \ll \phi_1$ , eq 7 can be approximated by

$$n_1^* = \exp(-\phi_1 \phi_1^*)[1 - \phi_2(\phi_2^* + g_1^*)] \tag{30}$$

$$n_2^* = \alpha \exp(\alpha \phi_r \phi_1^*) [1 + \alpha \phi_r (\phi_2^* + g_2^*)]$$
 (31)

If both  $-\phi_r(\phi_2^* + g_1^*)$  and  $\alpha\phi_r(\phi_2^* + g_2^*)$  can be treated as perturbed terms, then both eqs 30 and 31 can be further approximated by a linear expression. Therefore, in terms of scaled symbols, eqs 8 and 9 become

$$\nabla^{*2}\phi_{1}^{*} = -\frac{(\kappa a)^{2}}{(1+\alpha)\phi_{r}}[\exp(-\phi_{r}\phi_{1}^{*}) - \exp(\alpha\phi_{r}\phi_{1}^{*})] - Q_{\text{fix}}$$

$$\nabla^{*2}\phi_1^* = -\frac{(\kappa a)^2}{(1+\alpha)\phi_r} [\exp(-\phi_r \phi_1^*) - \exp(\alpha \phi_r \phi_1^*)]$$

$$b \le r \le c \quad (33)$$

In these expressions,  $\kappa^{-1} = [\epsilon kT/\sum n_{j0}(ez_j)^2]^{1/2}$  is the Debye length,  $\phi_r = z_1 e \zeta_a/kT$  is the scaled surface potential, and  $Q_{\rm fix} = \rho_{\rm fix} a^2/\epsilon \zeta_a$  is the scaled fixed charge density. The boundary conditions associated with eqs 32 and 33 are

$$\phi_1^* = 1 \qquad r^* = 1 \tag{34}$$

$$\phi_1^*|_{r^*=h^{-1}/a} = \phi_1^*|_{r^*=h^{+1}/a} \qquad r^* = b/a$$
 (35)

$$\frac{\partial \phi_1^*}{\partial r^*}\Big|_{r^*=b^{-/a}} = \frac{\partial \phi_1^*}{\partial r^*}\Big|_{r^*=b^{+/a}} \qquad r^* = b/a \tag{36}$$

$$\frac{\partial \phi_1^*}{\partial r^*} = 0 \qquad r^* = c/a \tag{37}$$

It can be shown that the corresponding governing equation for  $\phi_2^*$  is

$$\nabla^{*2}\phi_{2}^{*} = -\frac{(\kappa a)^{2}}{(1+\alpha)\phi_{r}}\{[\exp(-\phi_{r}(\phi_{1}^{*}+\phi_{2}^{*}+g_{1}^{*})) -$$

$$\exp(\alpha\phi_r(\phi_1^* + \phi_2^* + g_2^*))] - [\exp(-\phi_r\phi_1^*) - \exp(\alpha\phi_r\phi_1^*)]\}$$
(38)

and the associated boundary conditions are

$$\frac{\partial \phi_2^*}{\partial r^*} = 0 \qquad r^* = 1 \tag{39}$$

$$\phi_2^*|_{r^*=h/a} = \phi_2^*|_{r^*=h^+/a} \qquad r^* = b/a$$
 (40)

$$\frac{\partial \phi_2^*}{\partial r^*}|_{r^*=b/a} = \frac{\partial \phi_2^*}{\partial r^*}|_{r^*=b/a} \qquad r^*=b/a \tag{41}$$

$$\frac{\partial \phi_2^*}{\partial r^*} = -E_z^* \cos \theta \qquad r^* = c/a \tag{42}$$

It can be shown that  $g_1^*$  and  $g_2^*$  satisfy

$$\nabla^{*2}g_1^* - \phi_r \nabla^* \phi_1^* \cdot \nabla g_1^* = Pe_1 \mathbf{v}^* \cdot \nabla \phi_1^* + Pe_1 \mathbf{v}^* \cdot \nabla \phi_2^* + Pe_1 \mathbf{v}^* \cdot \nabla g_1^* + \phi_r \nabla^* \phi_2^* \cdot \nabla^* g_1^* + \phi_r \nabla^* g_1^* \cdot \nabla^* g_1^*$$
(43)

$$\nabla^{*2}g_{2}^{*} + \alpha\phi_{r}\nabla^{*}\phi_{1}^{*}\cdot\nabla g_{2}^{*} = Pe_{2}\mathbf{v}^{*}\cdot\nabla^{*}\phi_{1}^{*} + Pe_{2}\mathbf{v}^{*}\cdot\nabla\phi_{2}^{*} + Pe_{2}\mathbf{v}^{*}\cdot\nabla g_{2}^{*} - \alpha\phi_{r}\nabla^{*}\phi_{2}^{*}\cdot\nabla^{*}g_{2}^{*} - \alpha\phi_{r}\nabla^{*}g_{2}^{*}\cdot\nabla^{*}g_{2}^{*}$$
(44)

where  $Pe_j = U_E a/D_j$  is the electric Peclet number for ionic species j. The boundary conditions associated with eqs 43 and 44 are

$$\frac{\partial g_j^*}{\partial r^*} = 0$$
  $r^* = 1$   $j = 1,2$  (45)

$$g_j^*|_{r^*=b\cdot/a} = g_j^*|_{r^*=b^+/a} \qquad r^*=b/a \qquad j=1,2 \quad (46)$$

$$\frac{\partial g_{j}^{*}}{\partial r^{*r^{*}=b\cdot/a}} = \frac{\partial g_{j}^{*}}{\partial r^{*}}|_{r^{*}=b^{+}/a} \qquad r^{*}=b/a \qquad j=1,2 \ \, (47)$$

$$g_i^* = -\phi_i^*$$
  $r^* = c/a$   $j = 1,2$  (48)

In terms of the scaled stream function  $\psi^*$ , the governing equation for the flow field becomes

$$\begin{split} E^{*4}\psi^* - (\lambda a)^2 E^{*2}\psi^* &= -\frac{(\kappa a)^2}{(1+\alpha)} \times \\ &\left[ \left( \frac{\partial g_1^*}{\partial r^*} n_1^* + \frac{\partial g_2^*}{\partial r^*} (\alpha n_2^*) \right) \frac{\partial \phi^*}{\partial \theta} - \left( \frac{\partial g_1^*}{\partial r^*} n_1^* + \frac{\partial g_2^*}{\partial r^*} (\alpha n_2^*) \right) \frac{\partial \phi^*}{\partial r^*} \right] \sin \theta \\ &a < r < b \ (49) \end{split}$$

$$E^{*4}\psi^* = -\frac{(\kappa a)^2}{(1+\alpha)} \left[ \left( \frac{\partial g_1^*}{\partial r^*} n_1^* + \frac{\partial g_2^*}{\partial r^*} (\alpha n_2^*) \right) \frac{\partial \phi^*}{\partial \theta} - \left( \frac{\partial g_1^*}{\partial r^*} n_1^* + \frac{\partial g_2^*}{\partial r^*} (\alpha n_2^*) \right) \frac{\partial \phi^*}{\partial r^*} \right] \sin \theta \qquad b < r < c \quad (50)$$

The corresponding boundary conditions are

$$\psi^* = -\frac{1}{2}r^{*2}U^* \sin^2 \theta$$
  $\frac{\partial \psi^*}{\partial r^*} = -r^*U^* \sin^2 \theta$   $r^* = 1 (51)$ 

$$\psi^*|_{r^*=b/a} = \psi^*|_{r^*=b/a} \qquad r^* = b/a$$
 (52)

$$\frac{\partial \psi^*}{\partial r^*}|_{r^*=b/a} = \frac{\partial \psi^*}{\partial r^*}|_{r^*=b/a} \qquad r^*=b/a \tag{53}$$

$$\frac{\partial^2 \psi^*}{\partial r^{*2}}|_{r^*=b'/a} = \frac{\partial^2 \psi^*}{\partial r^{*2}}|_{r^*=b'/a} \qquad r^* = b/a \qquad (54)$$

$$\left[\frac{\partial^3 \psi^*}{\partial r^{*3}} - (\lambda a)^2 \frac{\partial \psi^*}{\partial r^*}\right]_{r^*=b/a} = \left[\frac{\partial^3 \psi^*}{\partial r^{*3}}\right]_{r^*=b^{+/a}} \quad r^* = b/a \quad (55)$$

$$\psi^* = 0$$
  $\left(\frac{\partial^2}{\partial r^{*2}} - \frac{2}{r^{*2}}\right)\psi^* = 0$   $r^* = c/a$  (56)

where the dimensionless group  $(\lambda a)^2 = (\gamma a^2/\eta)$  is a measure for the friction coefficient of the membrane layer.

The present problem can be made one-dimensional by applying the method of separation of variables. If all the perturbed variables in eqs 38–56 are linearized, then it can be shown that  $\phi_2^* = \Phi_2(r)\cos\theta$ ,  $g_1^* = G_1(r)\cos\theta$ ,  $g_2^* = G_2(r)\cos\theta$ , and  $\psi^* = \Psi(r)\sin^2\theta$ , and  $\Phi_2$ ,  $G_1$ , and  $G_2$  satisfy

$$L^{2}\Phi_{2} - \frac{(\kappa \alpha)^{2}}{(1+\alpha)} [\exp(-\phi_{r}\phi_{1}^{*}) + \alpha \exp(\alpha\phi_{r}\phi_{1}^{*})]\Phi_{2} = \frac{(\kappa \alpha)^{2}}{(1+\alpha)} [\exp(-\phi_{r}\phi_{1}^{*})G_{1} + \alpha \exp(\alpha\phi_{r}\phi_{1}^{*})G_{2}]$$
(57)

$$L^{2}G_{1} - \phi_{r}^{2} \frac{d\phi_{1}^{*}}{dr^{*}} = Pe_{1}\phi_{r}^{2}v_{r}^{*} \frac{d\phi_{1}^{*}}{dr^{*}}$$
 (58)

$$L^{2}G_{2} + \alpha \phi_{r}^{2} \frac{\mathrm{d}\phi_{1}^{*}}{\mathrm{d}r^{*}} = Pe_{2}\phi_{r}^{2}v_{r}^{*} \frac{\mathrm{d}\phi_{1}^{*}}{\mathrm{d}r^{*}}$$
 (59)

where

$$L^2 \equiv \frac{\mathrm{d}^2}{\mathrm{d}r^{*2}} + \frac{2}{r^*} \frac{\mathrm{d}}{\mathrm{d}r^*} - \frac{2}{r^{*2}}$$

The boundary conditions associated with eqs 57-59 are

$$\frac{\mathrm{d}\Phi_2}{\mathrm{d}r^*} = 0 \qquad r^* = 1 \tag{60}$$

$$\Phi_2|_{r^*=b\cdot/a} = \Phi_2|_{r^*=b^+/a} \qquad r^*=b/a \tag{61}$$

$$\frac{\mathrm{d}\Phi_2}{\mathrm{d}r^*}|_{r^*=b/a} = \frac{\mathrm{d}\Phi_2}{\mathrm{d}r^*}|_{r^*=b/a} \qquad r^*=b/a \qquad (62)$$

$$\frac{\mathrm{d}\Phi_2}{\mathrm{d}r^*} = -E_z^* \qquad r^* = c/a \tag{63}$$

$$\frac{dG_j}{dr^*} = 0 \qquad r^* = 1 \qquad j = 1,2 \tag{64}$$

$$G_j|_{r^*=b'/a} = G_j|_{r^*=b'/a}$$
  $r^*=b/a$   $j=1,2$  (65)

$$\frac{dG_j}{dr^*}|_{r^*=b/a} = \frac{dG_j}{dr^*}|_{r^*=b/a} \qquad r^* = b/a \qquad j = 1,2 \quad (66)$$

$$G_1 = -\Phi_2 \text{ and } G_2 = -\Phi_2 \qquad r^* = c/a$$
 (67)

For the flow field, we have

$$D^{4}\Psi - (\lambda a)^{2}D^{2}\Psi = -\frac{(\kappa a)^{2}}{1+\alpha} \left[ (n_{1}^{*}G_{1} + n_{2}^{*}G_{2}) \frac{\mathrm{d}\phi_{1}^{*}}{\mathrm{d}r^{*}} \right]$$

$$a < r < b \quad (68)$$

$$D^{4}\Psi = -\frac{(\kappa a)^{2}}{1+\alpha} \left[ (n_{1}^{*}G_{1} + n_{2}^{*}G_{2}) \frac{d\phi_{1}^{*}}{dr^{*}} \right] \qquad b < r < c \quad (69)$$

where

$$D^4 \equiv D^2 D^2 = \left(\frac{d^2}{dr^{*2}} - \frac{2}{r^{*2}}\right)^2$$

The boundary conditions associated with eqs 68 and 69 are

$$\Psi^* = -\frac{1}{2}r^{*2}U^*$$
 and  $\frac{d\Psi^*}{dr^*} = -r^*U^*$   $r^* = 1$  (70)

$$\Psi^*|_{r^*=b/a} = \Psi^*|_{r^*=b^+/a} \qquad r^* = b/a$$
 (71)

$$\frac{\mathrm{d}^2 \Psi^*}{\mathrm{d}r^{*2}} r^{*=b/a} = \frac{\mathrm{d}^2 \Psi^*}{\mathrm{d}r^{*2}} |_{r^*=b^{+/a}} \qquad r^* = b/a \qquad (72)$$

$$\frac{d\Psi^*}{dr^*}|_{r^*=b/a} = \frac{d\Psi^*}{dr^*}|_{r^*=b/a} \qquad r^* = b/a$$
 (73)

$$\left[\frac{\mathrm{d}^{3}\Psi^{*}}{\mathrm{d}r^{*3}} - (\lambda a)^{2} \frac{\mathrm{d}\Psi^{*}}{\mathrm{d}r^{*}}\right]_{r^{*}=b\cdot/a} = \left[\frac{\mathrm{d}^{3}\Psi^{*}}{\mathrm{d}r^{*3}}\right]_{r^{*}=b^{+}/a} \qquad r^{*} = b/a \tag{74}$$

$$\Psi^* = 0 \text{ and } \left(\frac{d^2}{dr^{*2}} - \frac{2}{r^{*2}}\right)\Psi^* = 0 \qquad r^* = c/a$$
 (75)

Sedimentation Potential. When a spherical particle bearing net negative charge falls down in the gravitational field, the double layer surrounding it is not spherical; there are excess positive mobile ions beneath the particle and excess negative mobile ions above it. The deformation of the double layer induces an electric field in the z-direction, which is opposite to the direction of the gravitational field. The electrical potential associated with this induced electric field is called the sedimentation potential, E, which can be evaluated based on the fact that the current arising from the sedimentation of a particle is balanced by that arising from the induced electric field. 16 At steady state, the sedimentation of the particle generates no net current, and the net flow of current across any horizontal plane vanishes. The current i arising from the sedimentation of a particle can be expressed as

$$\mathbf{i} = \sum_{j} z_{j} e n_{j} \mathbf{v_{j}} \tag{76}$$

The current across the horizontal plane,  $\theta = \pi/2$ , is

$$\langle i \rangle = 0 = 2\pi \int_{a}^{c} r i_{\theta} \, dr|_{\theta = \pi/2} = 2\pi \int_{a}^{c} r [\sum_{j=1}^{2} z_{j} e n_{j} v_{j\theta}] \, dr|_{\theta = \pi/2}$$
(77)

where subscript  $\theta$  denotes the  $\theta$ -component. The velocity of ionic species j,  $v_i$ , and that of liquid  $\mathbf{v}$  are related by

$$\mathbf{v_j} = \mathbf{v} - D_j \left( \frac{z_j e}{kT} \nabla \phi + \frac{\nabla n_j}{n_j} \right) \quad j = 1, 2$$
 (78)

Substituting this expression into eq 76, we obtain, in terms of scaled symbols,

$$\mathbf{i} = \frac{\epsilon^{3} \phi_{r}^{2}}{\eta \alpha^{3}} \left( \frac{kT}{z_{1}e} \right)^{3} \frac{(\kappa \alpha)^{2}}{(1+\alpha)} \left\{ \left[ \exp(-\phi_{r} \phi_{1}^{*}) - \exp(\alpha \phi_{r} \phi_{1}^{*}) \right] \mathbf{v}^{*} + \frac{1}{\phi_{r}} \left[ \frac{1}{Pe_{1}} \exp(-\phi_{r} \phi_{1}^{*}) \nabla^{*} g_{1}^{*} + \frac{\alpha}{Pe_{2}} \exp(\alpha \phi_{r} \phi_{1}^{*}) \nabla^{*} g_{2}^{*} \right] \right\}$$
(79)

The  $\theta$ -component of the current,  $i_{\theta}$ , can be expressed by

$$i_{\theta} = \frac{\epsilon^{3} \phi_{r}^{2}}{\eta a^{3}} \left(\frac{kT}{z_{1}e}\right)^{3} \frac{(\kappa a)^{2}}{(1+\alpha)} \{ [\exp(-\phi_{r}\phi_{1}^{*}) - \exp(\alpha\phi_{r}\phi_{1}^{*})] \} \frac{d\Psi}{dr^{*}} - \frac{1}{\phi_{r}} \left[\frac{1}{Pe_{1}} \exp(-\phi_{r}\phi_{1}^{*}) G_{1}^{*} \frac{\alpha}{Pe_{2}} \times \exp(\alpha\phi_{r}\phi_{1}^{*}) G_{2}^{*} \right] \frac{\sin \theta}{r^{*}}$$
(80)

This expression can be rewritten as

$$i_{\theta} = I_a I_{\theta}(r^*) \frac{\sin \theta}{r^*} \tag{81}$$

where

$$I_a = \frac{\epsilon^3 \phi_r^2}{na^3} \left(\frac{kT}{z_1 e}\right)^3 \frac{(\kappa a)^2}{(1+\alpha)}$$
(82)

$$I_{\theta} = \left\{ [\exp(-\phi_{r}\phi_{1}^{*}) - \exp(\alpha\phi_{r}\phi_{1}^{*})] \frac{d\Psi}{dr^{*}} - \frac{1}{\phi_{r}} \left[ \frac{1}{Pe_{1}} \exp(-\phi_{r}\phi_{1}^{*}) G_{1}^{*} \frac{\alpha}{Pe_{2}} \exp(\alpha\phi_{r}\phi_{1}^{*}) G_{2}^{*} \right] \right\}$$
(83)

Substituting eq 81 into eq 77 gives

$$\langle i \rangle = 0 = 2\pi a^2 I_a \int_1^{c/a} I_{\theta}(r^*) dr^*$$
 (84)

For a simpler treatment, the present problem is decomposed into two subproblems. <sup>14</sup> In the first problem, a particle moves with a constant velocity in the absence of the induced electric field, and in the second problem, the particle is held fixed when the induced electric field is present. The current in the first problem can be expressed as

$$\langle i \rangle_1 = \delta U^* \tag{85}$$

where  $U^* = U/U_E$ , and U is the z-component of the terminal velocity. The current in the second problem can be expressed as

$$\langle i \rangle_2 = \beta E_z^* \tag{86}$$

where  $E^* = E_z a/\zeta_a$ , and  $E_z$  is the z-component of the induced electric field. Since the net current across the horizontal plane  $\theta = \pi/2$  vanishes, that is,  $\langle i \rangle = \langle i \rangle_1 + \langle i \rangle_2 = 0$ , the

<sup>(15)</sup> Lee, E.; Chu, J. W.; Hsu, J. P. J. Chem. Phys. 1999, 110, 11643. (16) Hunter, R. J. Foundations of Colloid Science, Vols. 1 & 2; Oxford University Press: London, 1989.

scaled sedimentation potential  $E_z^*/U^*$  is

$$\frac{E_z^*}{U^*} = -\frac{\delta}{\beta} \tag{87}$$

The terminal velocity of a particle can be determined from the fact that the sum of the external forces acting on it in the z-direction vanishes at the steady state. For the present case, these include the electric force,  $F_{Ez}$ , the hydrodynamic forces,  $F_{Dz}$ , and the gravitational force,  $F_g$ , and they can be expressed respectively as

$$F_{Ez} = \frac{4}{3}\pi\epsilon \zeta_a^2 \left(r^{*2} \left(\frac{\mathrm{d}\phi_1^*}{\mathrm{d}r^*}\right) \left(\frac{\mathrm{d}\Phi_2}{\mathrm{d}r^*}\right) - 2r^* \left(\frac{\mathrm{d}\phi_1^*}{\mathrm{d}r^*}\right) \Phi_2\right)_{r^* = b/a} = \frac{4}{3}\pi\epsilon \zeta_a^2 F_{Ez}^* \quad (88)$$

$$egin{aligned} F_{Dz} &= rac{4}{3}\pi\epsilon {\zeta_a}^2 \Big[ r^{*2} rac{ ext{d}}{ ext{d}r^*} (D^2 \Psi) - 2 r^* (D^2 \Psi) \Big]_{r^* = b/a} + \ &rac{4}{3}\pi\epsilon {\zeta_a}^2 rac{(\kappa a)^2}{(1+lpha)\phi_r} \{ r^{*2} [\exp(-\phi_r \phi_1^*) - e^{-2}] \} \Big]_{r^* = b/a} \end{aligned}$$

 $\exp(\alpha \phi_r \phi_1^*)]\Phi_2\}_{r^*=b/a}$ 

$$=\frac{4}{3}\pi\epsilon\zeta_{a}^{2}(F_{Dhz}^{*}+F_{DEez}^{*})=\frac{4}{3}\pi\epsilon\zeta_{a}^{2}F_{Dz}^{*} \tag{89}$$

$$F_{g} = -\frac{4}{3}\pi a^{3}(\rho_{p} - \rho_{f})g - V_{s}(\rho_{s} - \rho_{f})g \qquad (90)$$

with

$$F_{Ez}^* = \left(r^{*2} \left(\frac{\mathrm{d}\phi_1^*}{\mathrm{d}r^*}\right) \left(\frac{\mathrm{d}\Phi_2}{\mathrm{d}r^*}\right) - 2r^* \left(\frac{\mathrm{d}\phi_1^*}{\mathrm{d}r^*}\right) \Phi_2\right)_{r^* = b/a} \quad (91)$$

$$F_{Dhz}^* = \left[ r^{*2} \frac{\mathrm{d}}{\mathrm{d}r^*} (D^2 \Psi) - 2r^* (D^2 \Psi) \right]_{r^* = b/a}$$
 (92)

$$\begin{split} F_{Dez}^* &= \frac{\left(\kappa a\right)^2}{(1+\alpha)\phi_r} \{r^{*2} [\exp(-\phi_r \phi_1^*) - \\ &\quad \exp(\alpha \phi_r \phi_1^*)] \Phi_2 \}_{r^* = b/a} \end{split} \tag{93}$$

In these expressions,  $\rho_f$ ,  $\rho_p$ , and  $\rho_s$  are respectively the densities of the fluid, the rigid core, and the membrane layer. We have  $F_{Dz} + F_{Ez} + F_g = 0$ , or

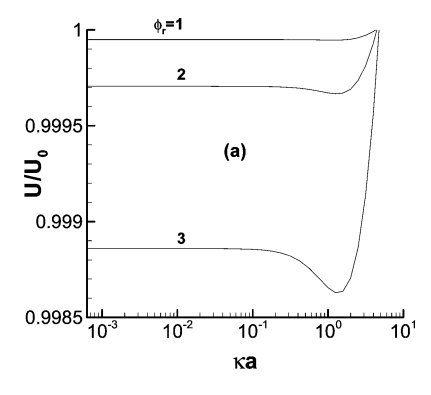
$$\frac{4}{3}\pi\epsilon\zeta_{a}^{2}(F_{Ez}^{*}+F_{Dhz}^{*}+F_{Dez}^{*})-\frac{4}{3}\pi a^{3}(\rho_{p}-\rho_{f})g-V_{s}(\rho_{s}-\rho_{f})g=0\ \ (94)$$

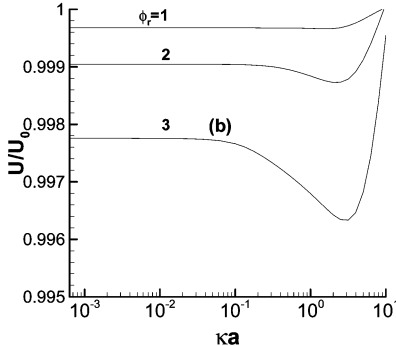
where  $V_s$  is the effective volume of the membrane layer. The term in the first parenthesis of this expression can be rewritten as  $f_1'U^* + f_2'E^*$ , where  $f_1'$  and  $f_2'$  are respectively the sum of the forces in problems 1 and 2. The sedimentation velocity can be expressed as

$$U = \frac{(4/3)\pi a^{3}(\rho_{p} - \rho_{f})g + V_{s}(\rho_{s} - \rho_{f})g}{(4/3)\pi\eta a} \left[f_{1}' - \frac{\delta}{\beta}f_{2}'\right]^{-1}$$

$$= \frac{c^{3}[\phi_{p}(\rho_{p} - \rho_{f}) + \phi_{s}(\rho_{s} - \rho_{f})]g}{\eta a} \left[f_{1}' - \frac{\delta}{\beta}f_{2}'\right]^{-1}$$
(95)

where  $\phi_p = (a/c)^3$  and  $\phi_s = V_s/(4\pi c^3/3)$  are respectively the volume fraction of the rigid core and the effective volume of the membrane layer. For convenience, the terminal





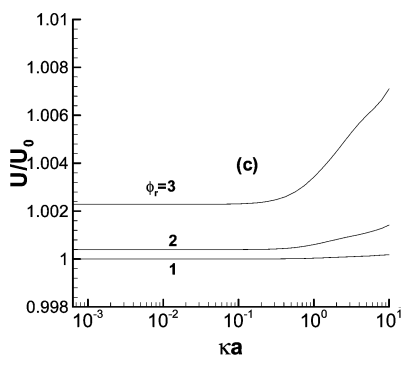


**Figure 2.** Variation of scaled sedimentation velocity  $U/U_0$  as a function of  $\kappa a$  at various  $\phi_r$  and  $Q_{\rm fix}$  for the case when  $\lambda a=10$  and H=0.421875: (a)  $Q_{\rm fix}=0$ , (b)  $Q_{\rm fix}=20$ , (c)  $Q_{\rm fix}=-20$ .

velocity of a sphere with uncharged membrane layer  $U_0$  is used as a reference velocity in subsequent discussions.

#### **Results and Discussion**

The sedimentation behavior of a particle is examined through numerical simulation. The governing equations and the associated boundary conditions are solved numerically by a pseudo-spectral method based on Chebyshev polynomials, which has been justified to be an efficient approach for electrokinetic phenomena of the present type. The For illustration, an aqueous KCl solution is chosen as a model system, and the following values are used:  $T=298.15~{\rm K}, \epsilon_r=6.954\times10^{-10}~{\rm F/m}, \eta_0=8.904\times10^{-3}~{\rm P}, \rho_f=0.99704~{\rm g/cm^3}, Pe_1=Pe_2=0.01, \rho_s=\rho_p=1.05~{\rm g/cm^3}, d/a=0.5, Z_1=Z_{K^+}=1, Z_2=Z_{K^-}=-1, D_1=D_{K^+}=1.962297\times10^{-5}~{\rm cm^2/s}, and D_2=D_{{\rm Cl}^-}=2.037051\times10^{-5}~{\rm cm^2/s}.$ 

Influence of Double-Layer Thickness. Figure 2 shows the variation of the scaled sedimentation velocity  $U/U_0$  as a function of double-layer thickness  $\kappa a$  at various fixed charge densities  $Q_{\rm fix}$ . Let us consider first the results shown in Figure 2a where the membrane layer of a particle is uncharged ( $Q_{\rm fix}=0$ ). This figure indicates that  $U/U_0$ 

<sup>(17)</sup> Canuto, C.; Hussaini, M. Y.; Quarteroni, A.; Zang T. A. Spectral Method in Fluid Dynamics; Springer-Verlag: Berlin, 1988.

approaches a constant as  $\kappa a \rightarrow 0$ . This is because if  $\kappa a \rightarrow$ 0, the double layer surrounding a particle is infinitely thick, and the mobile ions are uniformly distributed in the cavity. In this case, the sedimentation of a particle is influenced by the hydrodynamic force and the gravitational force only. If  $\kappa a$  is sufficiently large, the effect of doublelayer polarization comes into play. In this case, because the deformed double layer yields an induced electric field, which is in the z-direction, the sedimentation velocity declines. Note that if the double layer becomes thinner than the cavity radius, the absolute value of the potential gradient increases with the increase in  $\kappa a$ , and the distribution of ionic species in the cavity becomes more nonuniform. The latter provides a driving force for liquid flow, which decelerates the sedimentation of a particle. If κα increases further, the internal electric field arising from the potential gradient near the rigid core of a particle becomes stronger, which makes it more difficult for the double layer to deform. The competition between the effect of double-layer polarization and that of the internal electric field leads to a local minimum in  $U/U_0$  as  $\kappa a$  varies, as can be seen in Figure 2a. This local minimum may disappear if  $\phi_r$  is sufficiently low. This is because the effect of doublelayer polarization is significant only if  $\phi_r$  is sufficiently high and, furthermore, because the higher the  $\phi_r$ , the stronger the induced electric field and, therefore, the smaller the  $U/U_0$ . After passing the local minimum,  $U/U_0$ increases with the increase in  $\kappa a$ , and the higher the  $\phi_r$ , the faster the rate of increase of  $U/U_0$ . This is because if  $\kappa a$  is sufficiently large, the effect of double-layer polarization is insignificant, and the internal electric field dominates the behavior of a particle. In Figure 2b the membrane layer of a particle is positively charged. The behavior of  $U/U_0$  in this figure is similar to that observed in Figure 2a for the case when the membrane layer is free of fixed charge. Since the surface of the core of the particle is also positively charged, the presence of the membrane layer is equivalent to raising  $\phi_r$  to a higher level. As can be seen in Figure 2b, this is reflected by the fact that the influence of double-layer polarization occurs at a smaller  $\kappa a \ (\simeq 10^{-2})$  compared with that when the membrane layer if free of fixed charge. The variation of  $U/U_0$  when the membrane layer is negatively charged is illustrated in Figure 2c. In this case, although  $U/U_0$  also approaches a constant as  $\kappa a \rightarrow 0$ , it does not have a local minimum as  $\kappa a$  varies. This is because the induced electric field arising from double-layer polarization is in the same direction as that of sedimentation. That is, double-layer polarization has the effect of accelerating the sedimentation of a particle. In this case, the higher the  $\phi_r$ , the larger the  $U/U_0$ . For a fixed  $\phi_r$ ,  $U/U_0$  increases with the increase in  $\kappa a$ , as expected.

The simulated variation of the scaled sedimentation potential  $E^*/U^*$  for the case of Figure 2 is presented in Figure 3. This figure reveals that, regardless of the charged conditions of the membrane layer of a particle,  $E^*/U^*$ approaches a constant for both  $\kappa a \to 0$  and  $\kappa a \to \infty$ . The former is because if the double layer is infinitely thick, the ionic species are distributed uniformly in the cavity, and the equilibrium potential becomes independent of  $\kappa a$ . The latter arises from the fact that if  $\kappa a$  is large, doublelayer polarization is compressed by the internal electric field, and therefore, the sedimentation potential is no longer sensitive to the effect of double-layer polarization. For the case when the membrane layer of a particle is either free of fixed charge or positively charged, if  $\phi_r$  is sufficiently high,  $E^*/U^*$  has a local maximum as  $\kappa a$  varies, which is consistent with the result of Lee et al. 15 for the case of rigid particles and can be explained by the

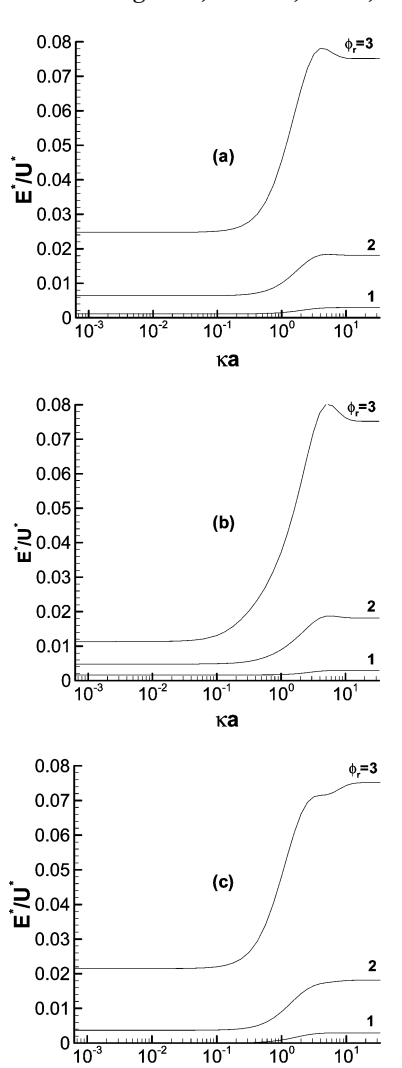
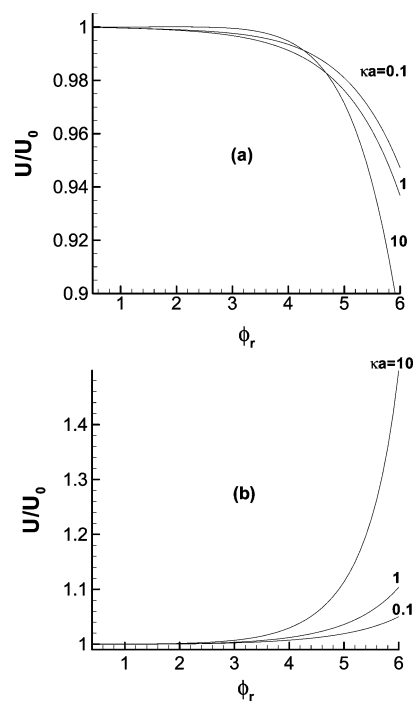


**Figure 3.** Variation of scaled sedimentation potential  $E^*/U^*$  as a function of  $\kappa a$  for the case of Figure 2.

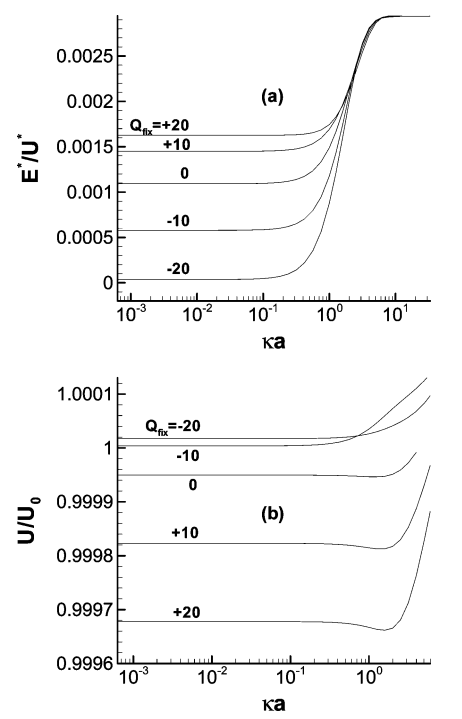
competition between the effects of double-layer polarization and the internal electric field. If the membrane layer is negatively charged, because the induced electric field has the same direction as that of the gravitational field, the local maximum does not appear, and  $E^*/U^*$  increases monotonically with  $\kappa a$ .

Influence of Surface Potential. The influence of the surface potential of the rigid core of a particle on its sedimentation velocity at various  $\kappa a$  is illustrated in Figure 4 for different  $Q_{\rm fix}$ . Figure 4a reveals that for the case when the membrane layer of a particle is positively charged, the scaled sedimentation velocity  $U/U_0$  declines with the increase in  $\phi_r$ . This is expected because the higher the  $\phi_r$ , the more significant the effect of double-layer polarization, which tends to retard the sedimentation of the particle. On the other hand, if the membrane layer is negatively charged,  $U/U_0$  increases with the increase in  $\phi_r$ , as is shown in Figure 4b. This is because the electric field induced by double-layer polarization is now in the same direction as that of sedimentation.

Influence of Fixed Charge Density. The simulated variations of the scaled sedimentation potential  $E^*/U^*$  and the scaled sedimentation velocity  $U/U_0$  as a function of  $\kappa a$  at various scaled fixed charge densities in the membrane layer of a particle  $Q_{\rm fix}$  are presented in Figure 5. Figure 5a reveals that for a fixed  $\kappa a$ ,  $E^*/U^*$  increases with  $Q_{\rm fix}$ . However, as  $\kappa a \to \infty$ , the influence of  $Q_{\rm fix}$  on

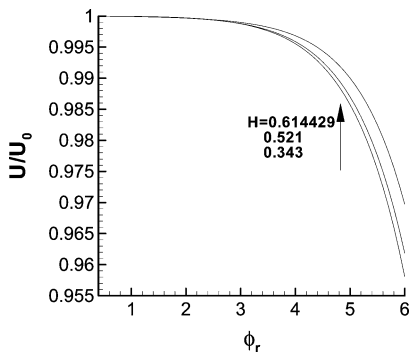


**Figure 4.** Variation of scaled sedimentation velocity  $U/U_0$  as a function of  $\phi_r$  at various  $\kappa a$  for the case when  $\lambda a=10$  and H=0.421875: (a)  $Q_{\rm fix}=20$ , (b)  $Q_{\rm fix}=-20$ .

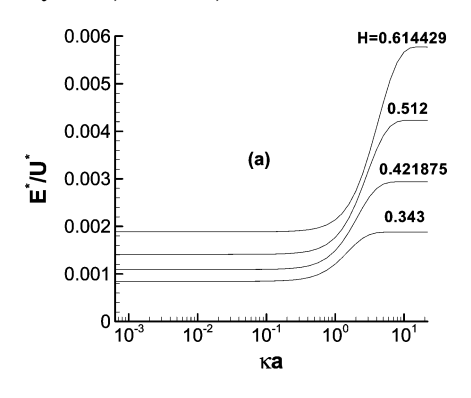


**Figure 5.** Variation of scaled sedimentation potential  $E^*/U^*$  (a) and scaled sedimentation velocity  $U/U_0$  (b) as a function of  $\kappa a$  at various  $Q_{\rm fix}$  for the case when  $\phi_r = 1.0$ ,  $\lambda a = 10$ , and H = 0.421875

 $E^*/U^*$  becomes unimportant, and  $E^*/U^*$  approaches a constant, which is independent of  $Q_{\rm fix}$ . The behavior of  $U/U_0$  as a function of  $\kappa a$  depends on the nature of  $Q_{\rm fix}$ . For  $Q_{\rm fix} \geq 0$ , the larger the  $Q_{\rm fix}$ , the smaller the  $U/U_0$ . Also,  $U/U_0$  has a local minimum as  $\kappa a$  varies, which can be explained by the effect of double-layer polarization. On the other hand, if  $Q_{\rm fix} < 0$ ,  $U/U_0$  increases monotonically with the increase in  $\kappa a$ . Furthermore, the relative magnitudes of  $U/U_0$  at different values of  $Q_{\rm fix}$  depend on



**Figure 6.** Variation of scaled sedimentation velocity  $U/U_0$  as a function of scaled surface potential  $\phi_r$  at various H for the case when  $Q_{\rm fix}=0$ ,  $\kappa a=1.0$ , and  $\lambda a=10$ .



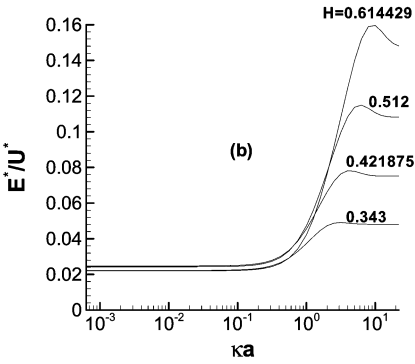


**Figure 7.** Variation of scaled sedimentation potential  $E^*/U^*$  as a function of  $\kappa a$  at various H for the case when  $Q_{\rm fix}=0$  and  $\lambda a=10$ : (a)  $\phi_r=1.0$ , (b)  $\phi_r=3.0$ .

the value of  $\kappa a$ . This is because the influence of double-layer polarization is insignificant when  $|Q_{\rm fix}|$  is small.

Boundary Effect. The boundary effect on the sedimentation velocity of a particle is illustrated in Figure 6, and that on its sedimentation potential is shown in Figure 7. For illustration, we assume that the membrane layer of a particle is free of fixed charge. In Figure 6, if  $\phi_r$  is low, that is, the effect of double-layer polarization is unimportant, the scaled sedimentation velocity  $U/U_0$  is almost independent of both  $\phi_r$  and H. On the other hand, if  $\phi_r$  is sufficiently high, the effect of double-layer polarization becomes significant. In this case, the larger the H, that is, the more important the boundary effect, the larger the  $U/U_0$ . Since double-layer polarization has the effect of retarding the sedimentation of a particle for the present case, this implies that the presence of the cavity has the effect of reducing the influence of double-layer polarization. This is because the liquid phase is confined by the cavity, and the larger the H, the smaller the space between the particle and the cavity available for the ionic cloud surrounding the former to deform. A similar result is also observed by Pujar and Zydney9 for the case of rigid

particles. Figure 7 reveals that if  $\phi_r$  is low, the scaled sedimentation potential  $E^*/U^*$  increases with the increase in  $\kappa a$  or the decrease in H. This is expected because the effect of double-layer polarization is insignificant if  $\phi_r$  is low. On the other hand, if  $\phi_r$  is sufficiently high,  $E^*/U^*$ exhibits a local maximum as  $\kappa a$  varies. Furthermore, the relative magnitude of  $E^*/U^*$  at different values of Hdepends on the value of  $\kappa a$ . These behaviors can be explained by the interaction between the effect of doublelayer polarization and that of the boundary.

### Conclusions

We show that the influence of the presence of a boundary on the sedimentation of a composite particle depends largely on the nature of the membrane layer of the particle, in particular, its charged conditions. This arises mainly from the effect of double-layer polarization. If the surface of the rigid core of a particle is positively charged, the main results can be summarized as follows: (a) If the membrane layer is either free of fixed charge or positively charged and the surface potential of the rigid core of the

particle is sufficiently high, the sedimentation velocity has a local minimum and the sedimentation potential has a local maximum as the thickness of the double layer varies. These local extrema do not appear when the membrane layer is negatively charged. (b) If the membrane layer of a particle is positively charged, its sedimentation velocity decreases with the increase in the surface potential of its rigid core. The reverse is true if the membrane layer of the particle is negatively charged. (c) For a fixed doublelayer thickness, the sedimentation potential increases with the density of fixed charge in the membrane layer. This trend becomes inappreciable as the double layer approaches infinitely thin. (d) The presence of a boundary has the effect of reducing the influence of double-layer polarization. The behavior of a particle when the surface of its rigid core is negatively charged can be inferred from the above observations.

**Acknowledgment.** This work is supported by the National Science Council of the Republic of China.

LA0476229